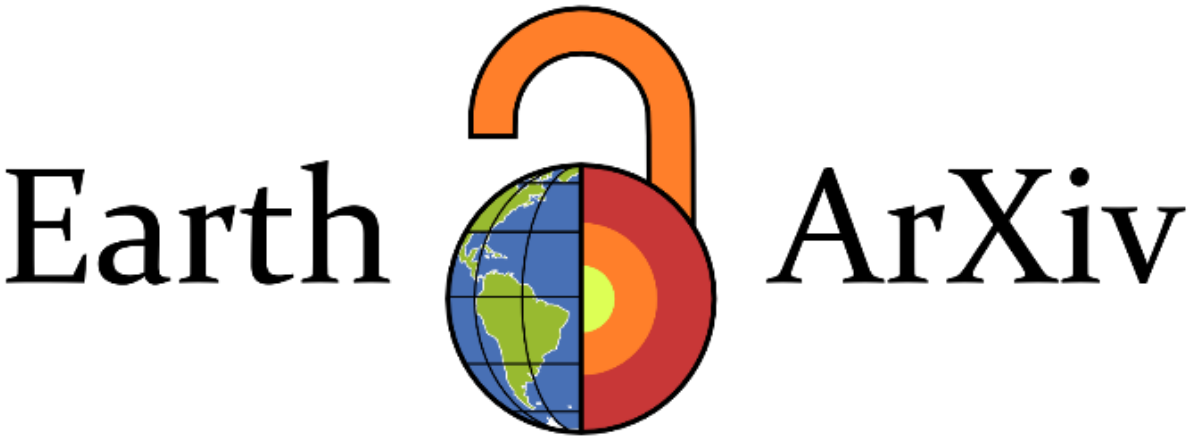

The Solar Paradox: Pure Social Diffusion and Competitive Resource Capture in Semi-Arid Irrigated Land Expansion

Tarek Gasmi[a], Ramzi Guesmi[b], Slim Ben Abdelbari[c], Ghaith Hammami[d]

[a] *University of Manouba, Campus Universitaire de la Manouba, 2010 Manouba, Tunisia*
[b] *University of Jendouba, Tunisia*
[c] *University of Sousse, Tunisia*
[d] *DataDoIt, Tunisia*

Abstract

Solar-powered irrigation is expanding rapidly across semi-arid regions, but the mechanisms through which this technology diffuses in informal groundwater economies—where the majority of wells operate without permits—remain poorly understood. We address this gap through a spatiotemporal analysis of 3,201 solar wells identified via satellite census in Sidi Bouzid, Tunisia, combined with 10,000 control points. Cox proportional hazards models reveal that terrain accessibility is the dominant spatial determinant: slope reduces the adoption hazard by 66% (HR = 0.339, $p < 0.001$), with proximity to urban centers (HR = 0.700) and lower elevation (HR = 0.718) also significant. Bass diffusion model estimation yields a near-zero innovation coefficient ($p = 0.001$) alongside a high imitation coefficient ($q = 0.679$)—the first documented case of $p \approx 0$ in agricultural technology diffusion, indicating a complete absence of institutional influence over the adoption process. We attribute this to a multi-layer governance failure in which legal barriers, fi-

nancial exclusion, and extension collapse block all formal technology transfer channels. A neighbor effects model reveals that higher local adopter density slows subsequent adoption (HR = 0.606, $p < 0.001$), creating an apparent paradox with the high aggregate imitation. We reconcile this through a Competitive Diffusion Framework distinguishing an aggregate-level Information Effect from a local-level Congestion Effect linked to aquifer stress. The Finance Law 2025's pivot to retroactive regularization of unauthorized wells confirms that informal diffusion has outpaced regulatory capacity, marking a transition from administrative exclusion to fiscal capture in Tunisia's groundwater governance.

Keywords: technology diffusion, Bass model, solar irrigation, groundwater governance, common-pool resources, spatial analysis, competitive diffusion, Tunisia

1. Introduction

The global expansion of solar-powered irrigation represents one of the most consequential land use transformations in semi-arid regions. By reducing the marginal cost of groundwater pumping to near zero, photovoltaic-driven systems remove the economic brake that fuel costs previously imposed on extraction, enabling unprecedented expansion of irrigated agriculture in water-scarce environments (Closas and Rap, 2017). This transformation sits at the nexus of three interconnected policy domains—water, energy, and food—creating trade-offs that conventional sectoral governance struggles to

manage (Hoff, 2011). While the water-energy-food nexus literature has extensively documented these trade-offs at the system level, a critical gap persists: how does solar irrigation actually diffuse among farming communities, and what determines whether this diffusion can be governed?

Understanding diffusion mechanisms is essential for policy design. If adoption is driven primarily by institutional channels—subsidies, extension services, credit programs—then regulators can steer the technology's spread through these levers, conditioning support on sustainable extraction practices. If, however, diffusion operates through informal social learning outside the reach of the state, regulators face a fundamentally different challenge: a self-organizing process that is resistant to conventional policy instruments.

This study investigates the diffusion of solar-powered irrigation in Sidi Bouzid, Tunisia, a semi-arid governorate where over 3,200 solar wells were installed between 2013 and 2025, the vast majority without official authorization. Tunisia presents a theoretically instructive case because it combines ambitious formal renewable energy targets (the *Plan Solaire Tunisien*) with a deeply informal groundwater economy in which 66.8% of deep wells operate without permits (ONAGRI, 2023) and aquifer exploitation reaches 149.7% of recharge. This conjunction creates conditions under which the standard assumption of technology diffusion theory—that both external (institutional) and internal (social) channels contribute to adoption—can be empirically tested against the alternative hypothesis that institutional channels are entirely inoperative.

We combine a satellite-based census of solar well installations with survival analysis (Cox proportional hazards) and diffusion modeling (Bass model) to address three research questions. First, what spatial and topographic factors determine where solar irrigation is adopted? Second, what is the relative contribution of external institutional influence versus internal social learning to the diffusion process? Third, how do local neighbor effects shape adoption dynamics as the technology saturates a shared resource base?

Our analysis yields three principal findings. First, adoption is overwhelmingly concentrated in time and space: 95.1% of wells were installed during a five-year "boom" (2021–2025), with a single year (2023) accounting for 53% of all installations. Second, Bass model estimation reveals that the innovation coefficient is indistinguishable from zero ($p \approx 0$), meaning that no measurable adoption was driven by government programs, bank loans, or extension services—a finding without precedent in the agricultural technology diffusion literature. Third, while aggregate spatial clustering confirms strong social learning, local neighbor density is associated with slower subsequent adoption (HR = 0.606), indicating emerging resource competition in dense adoption zones.

These findings contribute to the literature in three ways. Theoretically, we propose a Competitive Diffusion Framework that synthesizes Hägerstrand's (1967) spatial diffusion theory with Ostrom's (1990) common-pool resource framework, resolving the apparent paradox between high aggregate imitation and negative local neighbor effects. Empirically, we document the first case of

pure social diffusion ($p \approx 0$) in agricultural technology adoption, extending the Bass model literature into contexts of governance failure. For policy, we demonstrate that when formal channels are blocked, regulators lose all leverage over technology diffusion—a finding with direct implications for the Finance Law 2025 (Article 81, Loi n° 2024-48 (Loi n° 2024-48, 2024)), which represents Tunisia's first legislative acknowledgment that informal diffusion has outpaced regulatory capacity.

The remainder of this article proceeds as follows. Section 2 develops the Competitive Diffusion Framework. Section 3 provides study context, including the Authorization Trap that blocks formal channels and the recent Article 81 reform. Section 4 describes data collection and analytical methods. Section 5 presents results. Section 6 discusses theoretical and policy implications. Section 7 concludes.

2. Theoretical Framework

This study integrates three established theoretical traditions—technology diffusion, spatial contagion, and common-pool resource governance—into a unified framework we term the Competitive Diffusion Framework. This synthesis is motivated by a distinctive empirical puzzle: how can a technology exhibit strong aggregate imitation while simultaneously producing negative local neighbor effects? We argue that this paradox arises because solar-powered irrigation, unlike the consumer goods for which diffusion models were originally developed, is a rivalrous technology whose adoption physi-

cally degrades the shared resource base.

2.1. Technology diffusion and the Bass model

The Bass diffusion model (Bass, 1969) provides the canonical mathematical framework for understanding how innovations spread through a population. The model decomposes the instantaneous adoption rate into two components: an innovation effect (p), representing adoption driven by external forces such as subsidies, marketing, and extension services; and an imitation effect (q), representing adoption driven by social learning from prior adopters. When p is large relative to q, diffusion is policy-driven and can be steered by institutional levers. When q dominates, diffusion is self-organizing and resistant to top-down intervention.

Meta-analyses of Bass model applications across consumer durables consistently report average values of $p \approx 0.03$ and $q \approx 0.38$, yielding q/p ratios of approximately 13 (Sultan et al., 1990). Empirical studies of the choice of Bass coefficients confirm these benchmarks while highlighting sensitivity to estimation methods (Massiani, 2015). In agricultural contexts, Rogers (2003) documents typical p values of 0.01–0.03 and q values of 0.30–0.50, reflecting the dominant role of extension services and demonstration plots in driving adoption alongside peer learning. Even in extreme cases such as cellular phone diffusion, where network externalities amplify imitation, q/p ratios rarely exceed 168 (Baptista, 2000). Cross-country analyses of photovoltaic diffusion report similarly high imitation rates ($q \approx 0.3$–0.5) but with

measurable institutional effects ($p > 0$) reflecting subsidy regimes (Guidolin and Mortarino, 2010). A finding of $p \approx 0$ would thus represent a qualitative departure from the literature, implying a complete absence of institutional influence over the diffusion process.

Rogers (2003) identifies five attributes of innovations that shape their adoption rate: relative advantage, compatibility, complexity, trialability, and—critically—observability. Solar irrigation scores highly on both relative advantage (near-zero marginal pumping cost versus diesel) and observability (visible panel arrays adjacent to irrigated fields), creating conditions theoretically favorable to high imitation. However, Rogers's framework also predicts that external channels—mass media, extension agents—are most effective at the awareness stage, while interpersonal networks drive the persuasion stage. When external channels are absent, as we hypothesize for Tunisia's informal groundwater economy, the awareness function must also migrate to peer networks, producing a diffusion process entirely internal to the social system.

2.2. Spatial diffusion and the neighborhood effect

Hägerstrand (1967) pioneered the study of how innovations propagate through geographic space, introducing the concept of the Mean Information Field—the probability distribution of interpersonal communication contacts as a function of distance. His central insight was that information flows are denser among proximate individuals, producing spatially clustered adoption patterns that expand outward from initial adoption nodes over time. This

neighborhood effect predicts that the probability of adoption at any location is a function of the density and proximity of prior adopters in its vicinity.

Subsequent empirical work has refined this spatial mechanism. Conley and Udry (2010), studying fertilizer adoption in Ghana, demonstrated that farmers adjust inputs not in response to all neighbors but specifically to those whose outcomes were "surprisingly successful"—implying that the imitation channel transmits observed performance, not merely awareness. Foster and Rosenzweig (1995), analyzing the Indian Green Revolution, distinguished between learning by doing (own experience) and learning from others (neighbors' experience), showing that neighbors' accumulated experience functions as a quasi-public good that reduces the cost of adoption for latecomers. More recent work confirms the centrality of social networks: Genius et al. (2014) find that spatial effects and extension services jointly drive irrigation technology adoption in Crete, while Maertens and Barrett (2013) develop methods for measuring social network effects on agricultural technology uptake that account for endogenous network formation.

For solar irrigation, the spatial clustering prediction is amplified by two features of the technology: its high observability (panels are visible from considerable distances, including from satellite imagery) and its unambiguous performance signal (water flows or it does not). These attributes reduce the noise in the social learning channel, potentially explaining why imitation rates for solar irrigation may exceed those observed for technologies with more ambiguous returns, such as fertilizer or improved seed varieties.

2.3. Groundwater as a common-pool resource

The theoretical traditions reviewed above treat the diffusion environment as static—the resource base is implicitly assumed to be unaffected by adoption itself. This assumption holds for consumer goods (one person's purchase of a telephone does not reduce the telephone available to others) but fails for technologies that extract from a shared natural resource. Groundwater is a classic common-pool resource (CPR): it is subtractable (one farmer's extraction reduces the stock available to others) but difficult to exclude (aquifer boundaries do not respect property lines) (Ostrom, 1990).

Ostrom (1990) identified eight design principles for sustainable CPR governance, including clearly defined boundaries, effective monitoring, graduated sanctions, and conflict resolution mechanisms. Game-theoretic models confirm that cooperative groundwater management is difficult to sustain absent these institutional preconditions (Madani and Dinar, 2012; Edwards, 2016). When these principles are violated—as they systematically are in Tunisia's informal groundwater sector (Frija et al., 2014)—the "tragedy of the commons" (Hardin, 1968) becomes the expected equilibrium. Critically for diffusion dynamics, solar-powered pumping exacerbates the governance challenge by reducing the marginal cost of extraction to near-zero, removing the economic brake that diesel costs previously imposed on pumping volumes—the Jevons Paradox or rebound effect (Sears et al., 2018; Pfeiffer and Lin, 2014). Each additional solar well thus not only draws from the shared aquifer but also accelerates the rate at which the commons is depleted,

creating a feedback loop between adoption and resource degradation.

2.4. The Competitive Diffusion Framework

We synthesize these three traditions into a Competitive Diffusion Framework that resolves the apparent paradox between high aggregate imitation and negative local neighbor effects (Fig. 1). The framework posits two opposing spatial forces operating at different scales:

The **Information Effect** (+) operates at the aggregate level. Consistent with Hägerstrand (1967) and the Bass imitation mechanism, proximity to prior adopters reduces uncertainty, demonstrates viability, and provides access to informal knowledge about suppliers, installation, and operation. This force produces the population-level S-curve, spatial clustering, and a positive Moran's I statistic. It dominates during the early diffusion phases (pioneer and take-off) when adoption density is low and the resource base is not yet visibly stressed.

The **Congestion Effect** (−) operates at the local level. Consistent with CPR theory (Ostrom, 1990) and the economics of resource competition, spatial concentration of extraction accelerates aquifer drawdown, increases pumping depths, and raises costs for latecomers through hydrological interference (overlapping cones of depression). A complementary behavioral mechanism—strategic delay, whereby potential adopters observe neighbors' declining yields or operational problems before committing—may reinforce the physical congestion signal. Together, these forces produce negative local

neighbor effects—a hazard ratio below unity for neighbor density—indicating that locations surrounded by many prior adopters experience slower subsequent adoption. The Congestion Effect dominates during the later diffusion phases (saturation) when preferred sites are exhausted and aquifer stress becomes observable.

This framework draws on and extends Bandiera and Rasul's (2006) finding of an inverse-U relationship between adoption probability and network size in Mozambique, where social effects are positive at low adoption density and turn negative at high density. Our contribution is to ground this non-linearity in the physical properties of the resource: it is the rivalrous, subtractable nature of groundwater that transforms what begins as mutually beneficial information sharing into competitive resource capture. The sharp temporal transition from explosive adoption to rapid decline—visible in the 2023–2025 data—provides real-time evidence of the phase transition the framework predicts.

The framework generates five testable hypotheses. *H1 (Terrain Accessibility):* adoption concentrates in locations with favorable terrain—flat slopes, low elevation, proximity to markets. *H2 (Temporal Concentration):* diffusion follows an S-curve with a pronounced pioneer–boom structure. *H3 (Pure Social Diffusion):* the innovation coefficient approaches zero ($p \approx 0$), with diffusion driven exclusively by imitation (q). *H4 (Governance Failure):* the near-zero p reflects systematic blockage of formal technology transfer channels. *H5 (Competitive Diffusion):* local neighbor density has a negative effect

on adoption, reflecting the Congestion Effect, even as aggregate spatial clustering confirms the Information Effect.

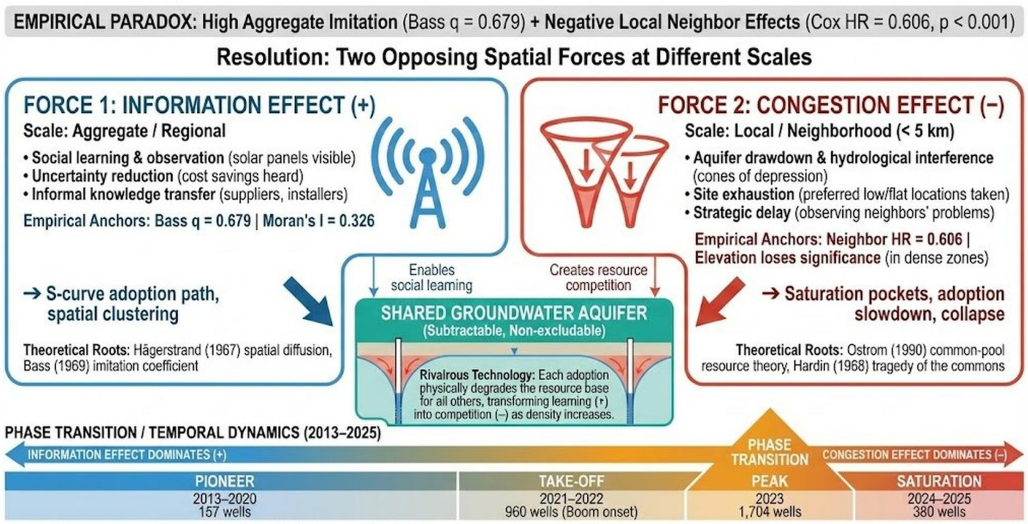

Figure 1: The Competitive Diffusion Framework. The framework resolves the empirical paradox between high aggregate imitation (Bass $q = 0.679$, Moran's $I = 0.326$) and negative local neighbor effects (Cox HR = 0.606) by distinguishing two opposing spatial forces. The Information Effect (+) operates at the aggregate level, producing the population-level S-curve and spatial clustering. The Congestion Effect (−) operates at the local level, slowing adoption in dense clusters as aquifer stress intensifies. The phase transition from Information-Effect dominance (Pioneer and Take-Off, 2013–2022) to Congestion-Effect dominance (Saturation, 2023–2025) is evidenced by the sharp collapse from 1,704 installations in 2023 to 380 in 2024–2025.

3. Study Context

3.1. The Sidi Bouzid governorate

Sidi Bouzid governorate (34.0°–35.2°N, 9.0°–10.0°E) lies in central Tunisia's semi-arid steppe zone, spanning approximately 7,400 km^2 of topographically varied terrain ranging from low-lying alluvial plains to elevated piedmont.

Mean annual precipitation is 200–350 mm, concentrated in the October–March wet season (Ministère de l'Agriculture, 2020), making rainfed agriculture marginal and groundwater-dependent irrigation essential for commercial crop production. The dominant agricultural systems include olive and almond orchards, open-field vegetable production, and livestock fodder—all highly dependent on groundwater (Elloumi, 2018). The aquifer exploitation rate has reached 149.7% of estimated recharge (ONAGRI, 2023), placing the governorate among the most critically overexploited groundwater basins in North Africa.

Sidi Bouzid is also the symbolic and political epicenter of the 2011 Tunisian revolution. The post-revolutionary period brought a sustained weakening of state authority in rural areas, with regulatory enforcement becoming effectively optional in a region where agricultural livelihoods are the sole economic anchor. This governance vacuum set the stage for the explosive, unregulated adoption of solar-powered irrigation that is the subject of this study.

3.2. The Authorization Trap

Understanding why the innovation coefficient should approach zero in this context requires examining the institutional architecture that blocks formal technology transfer. Tunisia's groundwater is governed by the 1975 *Code des Eaux* (Loi n° 75-16, 1975), which requires official authorization for any extraction from deep aquifers. In designated safeguard zones—including much of Sidi Bouzid—the regional agricultural development agencies (*Commissari-*

ats Régionaux de Développement Agricole, CRDAs) have imposed moratoria on new drilling permits. Yet enforcement collapsed after 2011: nationally, 32,575 deep wells operate without authorization, representing 66.8% of all deep boreholes (ONAGRI, 2023).

This creates what we term the "Authorization Trap"—a multi-layer governance failure that systematically excludes the majority of farmers from formal support channels. The mechanism operates through three reinforcing barriers. First, a *legal barrier*: the Tunisian state, through ANME and the agricultural investment agency APIA, offers subsidies covering up to 50% of solar installation costs, but eligibility requires a valid water extraction authorization—the very permit the CRDAs refuse to issue in overexploited zones. Second, *financial exclusion*: banks require well authorization to process equipment loans; without it, the installation is "unbankable," forcing farmers into cash purchases from savings or informal credit. Survey data from a GIZ/ANME assessment found that 0% of sampled solar adopters utilized formal bank credit—63% relied on own funds, 38% on supplier credit (GIZ/ANME, 2019). Third, *extension collapse*: state extension agents cannot officially promote technology for illegal infrastructure; ministry programs exclude unlicensed wells; and the private installers who fill the gap operate on reputation within informal trust networks rather than technical standards.

The result is a complete severance of the formal innovation channel. No subsidy reaches the farmer; no bank markets the technology; no extension agent demonstrates it. In Bass model terms, every institutional mechanism

that normally generates positive p is blocked, generating a clear prediction: if the Authorization Trap operates as theorized, the innovation coefficient should approach zero, with diffusion migrating entirely to the informal imitation channel (q) and propagating through neighbor-to-neighbor observation and word-of-mouth. The accumulated consequence—tens of thousands of wells operating outside any regulatory framework—eventually forced a legislative response.

3.3. From prohibition to taxation: Article 81

The governance landscape shifted in December 2024 with the passage of Article 81 of Loi n° 2024-48 (Loi n° 2024-48, 2024), published in *JORT* n° 149. This article establishes a formal mechanism for the "regularization of unauthorized deep agricultural wells" (*Régularisation des puits profonds non autorisés*), creating distinct fee categories for electrified wells and solar-equipped wells (2,000–2,500 TND for the latter). The very existence of a mass regularization pathway constitutes legislative confirmation that the Authorization Trap was not a theoretical construct but an empirical reality affecting tens of thousands of farmers.

We interpret Article 81 as marking a fundamental transition from *Administrative Exclusion* (2011–2024), wherein the state maintained a regulatory framework that criminalized the majority of its agricultural actors while tolerating their existence, to *Fiscal Capture* (2025–), wherein the state pivots from attempting to control diffusion to taxing its results. Whether this tran-

sition will restore positive innovation effects ($p > 0$) remains to be seen. For the innovation coefficient to become meaningfully positive, the state would need to link regularization to subsidy eligibility, create extension services for newly regularized wells, and integrate solar well owners into formal credit markets. Without these complementary measures, regularization represents a recognition of past informal diffusion rather than a driver of future formal diffusion.

3.4. The economic trigger: converging cost pressures

The temporal pattern of adoption reflects converging economic forces (Fig. 2). Global solar PV costs declined 93% from 2010 to 2023 (IRENA, 2024), making self-financed installation increasingly affordable. Simultaneously, diesel prices in Tunisia rose from 1.84 TND/L in 2022 to 2.53 TND/L in 2024, increasing the relative advantage of solar pumping. Olive oil farm-gate prices peaked at 27.5 TND/kg in 2023 before collapsing to 13.5 TND/kg in 2024 (ONH, 2024), first providing the capital for investment and then squeezing farmers into cost-minimization strategies. Meanwhile, the tripling of customs duties on solar equipment from 10% to 30% (Article 40, Loi n° 2023-13 (Loi n° 2023-13, 2023), effective January 2024) abruptly increased the capital cost of installation. The adoption response to these dynamics is documented in Section 5.1 (Fig. 4).

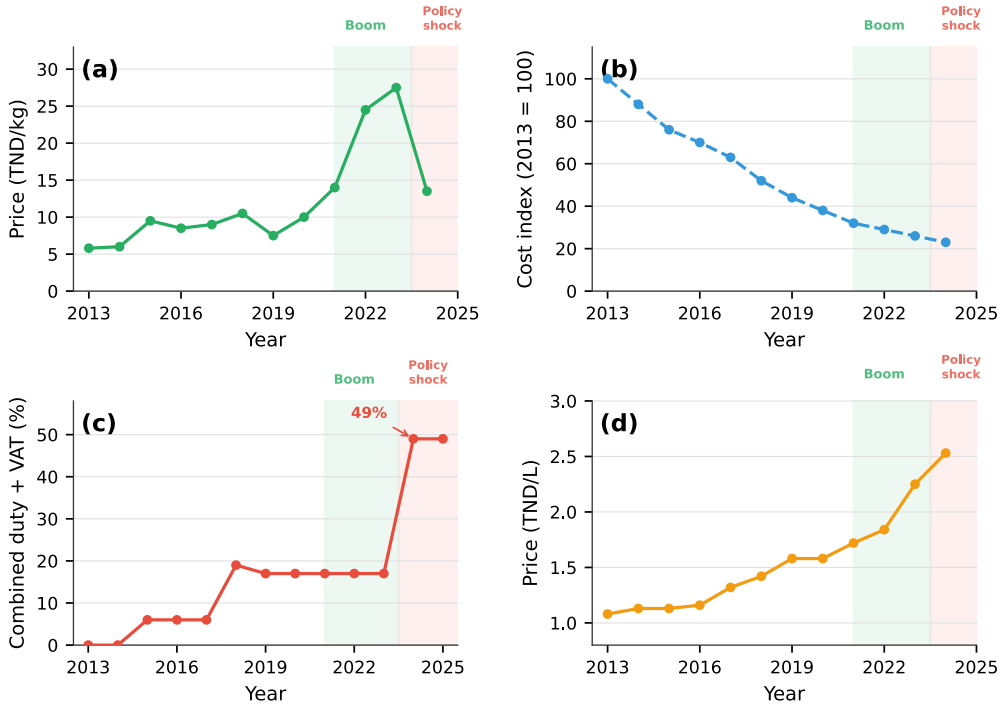

Figure 2: Economic context of solar well adoption, 2013–2025. (a) Olive oil farm-gate prices peaked at 27.5 TND/kg in 2023, providing investment capital. (b) Global solar PV costs declined 77% over the study period (IRENA, 2024). (c) Combined tax burden on solar equipment rose from 0% to 49% following the January 2024 customs duty tripling (Article 40, Loi nº 2023-13). (d) Diesel prices doubled from 1.08 to 2.53 TND/L, increasing the relative advantage of solar pumping. Green shading indicates the boom period (2021–2023); red shading indicates the protectionist policy shock (2024+). The adoption response to these economic dynamics is shown in Fig. 4. Sources: ONH/INS (olive), IRENA (solar), GlobalPetrolPrices (diesel), Loi de Finances (fiscal).

4. Data and Methods

4.1. Study area

The study focuses on Sidi Bouzid governorate in central Tunisia (Fig. 3). Section 3.1 provides a detailed description of the study area, its groundwater crisis, and the Authorization Trap governance mechanism that shapes diffusion dynamics.

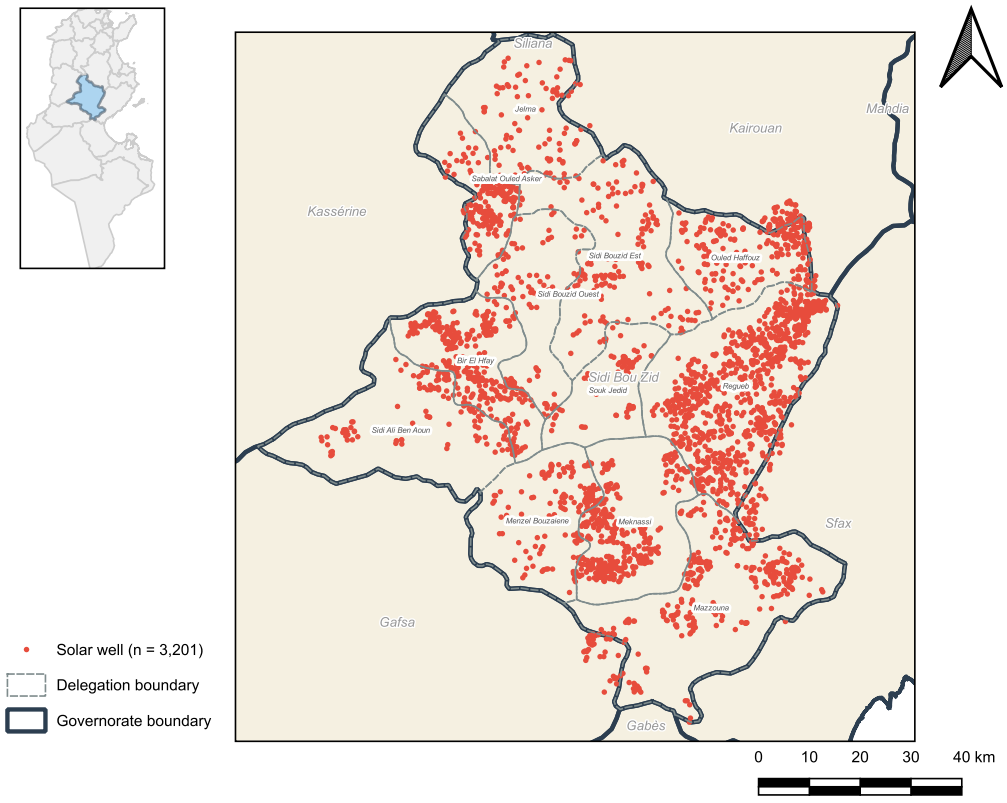

Figure 3: Study area map of Sidi Bouzid governorate, central Tunisia, showing administrative boundaries and the location of identified solar-powered irrigation wells ($n = 3{,}201$).

4.2. Data sources and variable construction

4.2.1. Solar well identification through satellite census

To reconstruct the spatiotemporal diffusion history of solar-powered irrigation in Sidi Bouzid, we conducted a systematic manual census using high-resolution satellite imagery. The three-month data collection campaign (June–August 2025) employed a 1 km $\times$ 1 km grid system to ensure exhaustive spatial coverage and prevent selection bias. Enumerators systematically scanned each grid cell using Google Earth Pro (Desktop Version 7.3), identifying solar panel installations adjacent to agricultural fields based on three visual heuristics: (i) *geometric signature*—dark blue/black rectangular arrays with high geometric regularity, distinct from irregular canopy cover or soil patches; (ii) *contextual association*—proximity (<50 m) to agricultural infrastructure such as water storage basins or irrigation distribution heads, to distinguish SPIS from residential or industrial solar installations; and (iii) *shadow analysis*—verification of panel tilt and elevation via shadow projection to distinguish ground-mounted arrays from surface water or flat tarps. For each identified installation, enumerators recorded precise coordinates (6 decimal places), estimated array surface area, and administrative sector (*Imada*).

Temporal reconstruction was achieved through the Historical Imagery Time-Slider tool in Google Earth Pro. The installation year was defined as the timestamp of the first available image in which the solar array is clearly visible. Observations with image gaps exceeding two years were flagged for

secondary cross-checking or excluded from time-series analysis to prevent temporal attribution bias. Portable solar kits with arrays smaller than 5 m^2 were systematically excluded to maintain consistency.

Quality assurance followed a multi-source triangulation protocol. A random sample of 10% of identified points was cross-referenced against ESRI World Imagery basemaps, which utilize different satellite passes than Google Earth, enabling verification of feature persistence under different lighting conditions and viewing angles. Features not confirmed as rigid structures in both sources were discarded. Inter-rater reliability was assessed through a blind double-coding experiment: five randomly selected 1 km^2 grid cells representing diverse terrain types (high-density olive groves, open field crops, rocky slopes) were independently re-scanned by a senior supervisor without access to the original dataset. Using a 15-meter spatial tolerance threshold, this procedure yielded 94.5% agreement on feature detection, with discrepancies concentrated among very small arrays near the 5 m^2 exclusion threshold.

The final dataset comprises 3,201 confirmed solar well locations with installation dates spanning 2013–2025. To construct a control sample representing potential but unrealized adoption sites, we generated 10,000 random points within agricultural areas—identified from MODIS land cover classification (Friedl et al., 2010)—that did not contain observable solar installations as of 2025. This case-control design (13,201 total observations: 3,201 events, 10,000 censored) enables estimation of factors associated with the timing and spatial distribution of adoption.

4.2.2. Predictor variables

We assembled a suite of geospatial predictor variables hypothesized to influence solar well adoption based on prior literature on agricultural technology diffusion and groundwater access (Table 1). All variables were extracted at each well and control location using Google Earth Engine (Gorelick et al., 2017).

Table 1: Descriptive statistics of predictor variables by adoption status.

Variable	Full Sample ($n = 13{,}201$)	Adopters ($n = 3{,}201$)	Non-Adopters ($n = 10{,}000$)	Difference
Topographic				
Elevation (m)	297 (151)	253 (112)	311 (159)	−58***
Slope (°)	3.32 (4.19)	1.91 (1.14)	3.77 (4.68)	−1.86***
TWI	4.62 (2.14)	4.87 (1.87)	4.54 (2.21)	+0.33***
Accessibility				
Travel time (min)	58.6 (33.8)	52.3 (28.4)	60.6 (35.4)	−8.3***
Socioeconomic				
Pop. density (pers/km^2)	0.40 (1.13)	0.45 (0.89)	0.38 (1.18)	+0.07**
Baseline NDVI	0.155 (0.045)	0.16 (0.03)	0.15 (0.04)	+0.01***

Notes: Values are mean (SD). Difference tested via two-sample t-test.
*** $p < 0.001$, ** $p < 0.01$.

Topographic variables were derived from the Shuttle Radar Topography Mission (SRTM) 30 m Digital Elevation Model: *elevation* (mean within 100 m buffer, meters), capturing variation in groundwater depth and pumping costs; *slope* (terrain gradient in degrees), reflecting drilling accessibility and irrigation feasibility; and the *Topographic Wetness Index* (TWI), a compound index of water accumulation potential calculated as $\ln(\alpha / \tan \beta)$,

where α is upslope contributing area and β is local slope.

Accessibility variables capture market integration and transaction costs: *travel time to nearest city* (friction-weighted travel time in minutes to urban centers with population >50,000), derived from the Malaria Atlas Project accessibility surface (Weiss et al., 2018).

Socioeconomic variables proxy for local economic conditions and information access: *population density* (persons/km^2) from WorldPop 2020 estimates at 1 km resolution, and *baseline NDVI* (mean Normalized Difference Vegetation Index from Landsat, 2010–2012), capturing pre-adoption agricultural productivity as a measure of agricultural potential.

4.2.3. Spatial neighbor variables

To test for social learning and local saturation effects, we constructed a spatially-lagged adoption variable: the count of solar wells installed before the focal well within a 5 km radius (*prior neighbors within 5 km*). This variable enables direct testing of whether adoption accelerates—or decelerates—in locations with more prior nearby adopters, as predicted by social learning and resource competition models respectively.

4.3. Analytical framework

Our analytical strategy employs three complementary methodological approaches to characterize the spatial determinants, temporal dynamics, and diffusion mechanisms of solar well adoption.

4.3.1. Survival analysis: Cox proportional hazards model

We model adoption timing using Cox proportional hazards regression, treating solar well installation as a "failure" event in survival analysis terminology. This approach accommodates both adopted locations (with known installation years) and non-adopted control locations (right-censored observations). The Cox model specifies the hazard of adoption at time t for location i as:

$$h_i(t) = h_0(t) \exp\big(\beta_1 X_{1i} + \beta_2 X_{2i} + \cdots + \beta_k X_{ki}\big) \tag{1}$$

where $h_0(t)$ is the unspecified baseline hazard function, $X_{1i} \ldots X_{ki}$ are predictor variables, and $\beta_1 \ldots \beta_k$ are coefficients to be estimated. The exponentiated coefficients $\exp(\beta)$ yield hazard ratios (HR), interpretable as the multiplicative change in adoption hazard associated with a one-standard-deviation increase in the predictor.

We define the time origin as 2012 (one year before first observed adoption) and measure time in years. Wells are assigned event times corresponding to their installation year minus 2012; control locations are right-censored at 2025 (end of the observation period). Continuous predictors were standardized to z-scores (mean = 0, SD = 1) to facilitate comparison of effect magnitudes across variables measured on different scales. Parameters were estimated via partial likelihood maximization using the `survival` package in R (Therneau, 2023), and we report hazard ratios with 95% confidence intervals and Wald-

test p-values.

To examine whether adoption drivers changed between the initial "pioneer" phase (2013–2020) and the subsequent "boom" phase (2021–2025), we estimated separate Cox models for each period. This time-stratified analysis also addresses potential violations of the proportional hazards assumption (see Section 4.4).

4.3.2. Diffusion modeling: Bass model

To characterize aggregate diffusion dynamics and distinguish between external innovation and internal imitation mechanisms, we fit the Bass diffusion model to the cumulative adoption time series (Bass, 1969). The Bass model decomposes the adoption rate into two components:

$$\frac{dN(t)}{dt} = \left[p + q\,\frac{N(t)}{K}\right]\left[K - N(t)\right] \tag{2}$$

where $N(t)$ is the cumulative number of adopters at time t, K is the market potential (carrying capacity), p is the coefficient of innovation (external influence from subsidies, marketing, extension services), and q is the coefficient of imitation (internal influence from social learning, peer observation). The ratio q/p indicates the relative importance of internal versus external influence, with higher values reflecting socially-driven diffusion.

Parameters were estimated via nonlinear least squares using the Levenberg–Marquardt algorithm (R package `minpack.lm`), applied to the integrated closed-form solution. We compared the full Bass model (3 parameters: p,

q, K) against two nested alternatives to formally test whether external innovation effects are statistically distinguishable from zero: (i) a pure logistic model (2 parameters: q, K; constraining $p = 0$), and (ii) a literature-constrained Bass model (2 parameters: q, K; fixing $p = 0.03$ per Sultan et al. 1990). Model selection was based on the Akaike Information Criterion (AIC), with $\Delta\text{AIC} > 10$ considered decisive evidence against the inferior model (Burnham and Anderson, 2002).

As a triangulation exercise, we also fit an equivalent epidemic (SIS) model formulation, which represents adoption as a contagion process with a transmission rate β analogous to the imitation coefficient. Agreement between the epidemic growth rate and the Bass imitation coefficient would strengthen confidence in the social contagion interpretation.

4.3.3. Spatial autocorrelation analysis

To formally test for spatial clustering in adoption patterns—a necessary condition for neighbor-based social learning—we computed Moran's I statistic on adoption status using k-nearest neighbors spatial weights ($k = 8$) (Anselin, 1995). Positive and statistically significant Moran's I indicates that adopted locations tend to be near other adopted locations more than expected under spatial randomness, consistent with localized diffusion processes.

4.4. Model diagnostics and robustness checks

We assessed the robustness of our findings through several complementary strategies. First, we evaluated Cox model stability across six alternative specifications: the baseline model with all standardized predictors (Model A); a reduced model excluding TWI to address potential multicollinearity with elevation (Model B); a model including a slope × elevation interaction term to test for nonlinear terrain effects (Model C); a categorical specification with quartile-coded predictors to relax functional form assumptions (Model D); a model stratifying the baseline hazard by land cover type (Model E); and a model with cluster-robust standard errors to account for spatial dependence (Model F). Coefficients varying by less than 20% across specifications were considered robust.

Second, to address the strong spatial clustering documented by Moran's I, we re-estimated the baseline Cox model using cluster-robust (sandwich) standard errors that allow for arbitrary within-cluster correlation (Lin and Wei, 1989). We partitioned the study area into 377 spatial clusters based on a geographic grid and computed robust variance estimates using the grouped jackknife (cluster sandwich) estimator. The ratio of robust to conventional standard errors—the SE inflation factor—quantifies the degree to which spatial dependence inflates uncertainty.

Third, the proportional hazards assumption was tested using Schoenfeld residuals (Grambsch and Therneau, 1994). Variables exhibiting significant time-dependence were addressed through time-stratified analysis and inter-

pretation noting that reported hazard ratios represent time-averaged effects.

Fourth, given the novelty of the $p \approx 0$ finding, we conducted extensive robustness checks on the Bass model: sensitivity analysis fixing K at values ranging from 1.0× to 2.0× maximum observed adoption, and an equivalent epidemic model as an independent triangulation.

Fifth, as a non-parametric complement to the Cox model, we estimated a Random Forest classification model (Breiman, 2001) predicting well presence versus control points. The model was trained on 9,234 observations using 500 trees with 3 variables considered at each split ($mtry = 3$), achieving an out-of-bag error rate of 19.6%. Variable importance was assessed via Mean Decrease in Accuracy and Mean Decrease in Gini impurity (Fig. A4). Because the model prioritizes overall classification accuracy, the class-specific error rate for wells (60.1%) was substantially higher than for controls (6.6%); variable importance rankings are nonetheless informative for identifying which environmental features most strongly differentiate well locations from the background landscape.

4.5. Software and reproducibility

All analyses were conducted in R (version 4.3.x). Key packages included `survival` for Cox models (including cluster-robust variance via the `cluster` argument), `minpack.lm` for nonlinear least squares, `randomForest` for variable importance analysis, `spdep` for spatial autocorrelation, `sf` for spatial operations, and `ggplot2` for visualization. Geospatial data extraction was

performed in Google Earth Engine (Gorelick et al., 2017).

5. Results

5.1. Descriptive patterns

The final sample comprises 13,201 observations: 3,201 identified solar wells and 10,000 randomly sampled control points within agricultural areas. Solar wells exhibited systematically different site characteristics compared to control locations (Table 1; Fig. 5). Adopters were located at lower elevations (253 ± 112 m vs. 311 ± 159 m, $p < 0.001$), on flatter terrain ($1.91 \pm 1.14°$ vs. $3.77 \pm 4.68°$, $p < 0.001$), and closer to urban centers (52.3 ± 28.4 min vs. 60.6 ± 35.4 min travel time, $p < 0.001$). These univariate differences suggest that adoption is spatially selective, concentrated in locations with favorable topographic and accessibility characteristics.

Adoption exhibited a highly concentrated temporal pattern. The "pioneer" phase (2013–2020) accounted for only 157 wells (4.9% of total), with annual installations rarely exceeding 50 units. The transition to the "boom" phase (2021–2025) was dramatic: 3,044 wells (95.1%) were installed in five years, with a single year—2023—accounting for 1,704 installations (53.2% of all wells). The subsequent decline to 308 wells in 2024 and 72 in early 2025 suggests an emerging saturation dynamic (Fig. 4). This hyper-concentration—95% of adoption occurring in 38% of the study period—is consistent with epidemic-style contagion where a slow initial seed phase triggers explosive but self-limiting growth.

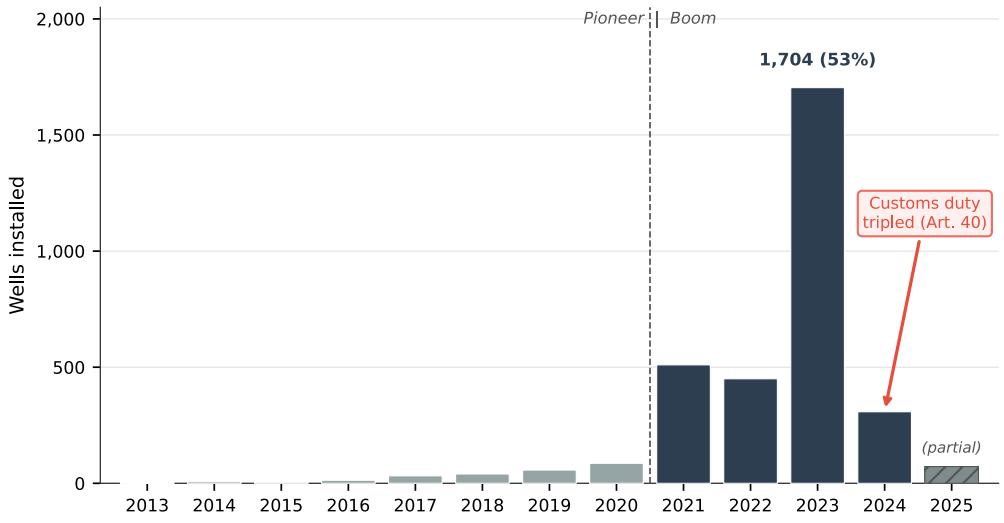

Figure 4: Annual solar well installations in Sidi Bouzid governorate, 2013–2025. The Pioneer phase (2013–2020, 157 wells, 4.9%) and Boom phase (2021–2025, 3,044 wells, 95.1%) are distinguished by shading. The 2023 peak (1,704 wells, 53% of total) coincides with maximum economic profitability. The 2024 collapse follows the tripling of customs duties on solar equipment (Article 40, Loi n° 2023-13 (Loi n° 2023-13, 2023)). The 2025 bar reflects partial-year data through August.

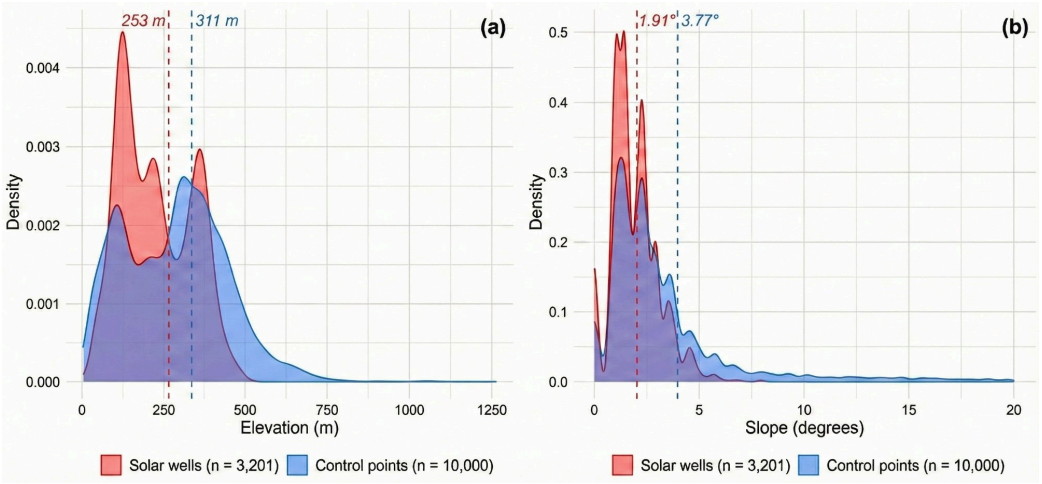

Figure 5: Density distributions of (a) elevation and (b) slope for solar well locations (n = 3,201) versus random control points (n = 10,000). Dashed vertical lines indicate group means. Solar wells concentrate at lower elevations (253 ± 112 m vs. 311 ± 159 m) and on flatter terrain ($1.91 \pm 1.14°$ vs. $3.77 \pm 4.68°$), consistent with the Cox model results (elevation HR = 0.718, slope HR = 0.339, both $p < 0.001$).

5.2. Spatial determinants of adoption

Cox proportional hazards regression revealed that terrain characteristics are the dominant predictors of adoption timing (Table 2; Fig. 6). Slope exhibited the strongest effect: a one-standard-deviation increase in slope (approximately 4.2°) was associated with a 66% reduction in adoption hazard (HR = 0.339, 95% CI: 0.300–0.384, $p < 0.001$). Travel time to the nearest city was the second-strongest predictor (HR = 0.700, 95% CI: 0.669–0.733, $p < 0.001$), indicating that market accessibility significantly accelerates adoption, likely reflecting access to equipment suppliers, information networks, and output markets. Elevation showed a similar pattern (HR = 0.718, 95% CI: 0.687–0.751, $p < 0.001$), with lower-lying areas—where water tables are shallower and existing agriculture is concentrated—adopting more rapidly.

Population density was negatively associated with adoption (HR = 0.785, 95% CI: 0.715–0.862, $p < 0.001$), suggesting that less densely populated areas, where extensive agriculture predominates, adopt faster. The Topographic Wetness Index showed a modest negative effect (HR = 0.866, 95% CI: 0.831–0.902, $p < 0.001$), indicating that locations with greater natural water accumulation potential adopt more slowly—consistent with reduced urgency for irrigation investment where surface moisture is naturally higher. Baseline NDVI showed a small positive association (HR = 1.045, 95% CI: 1.008–1.084, $p = 0.017$) under standard errors, but this effect was not robust to cluster-robust inference ($p = 0.164$; see Section 5.7) and should be interpreted with caution. Model concordance was 0.675 (SE = 0.005), indicating acceptable discriminative ability.

5.3. Temporal dynamics: pioneer versus boom

Time-stratified analysis revealed shifting adoption dynamics between the pioneer (2013–2020, $n = 157$ events) and boom (2021–2025, $n = 3{,}044$ events) periods (Table A2 in Appendix A). The slope constraint remained strong and stable across both phases (pioneer HR = 0.427; boom HR = 0.400; $\Delta = -6\%$), confirming that flat terrain is a non-negotiable physical requirement for solar well installation. In contrast, the elevation constraint relaxed substantially (pioneer HR = 0.587; boom HR = 0.720; $\Delta = +23\%$), suggesting that as diffusion accelerated, adoption expanded from optimal low-lying valley sites to higher, more marginal locations—a pattern consistent with

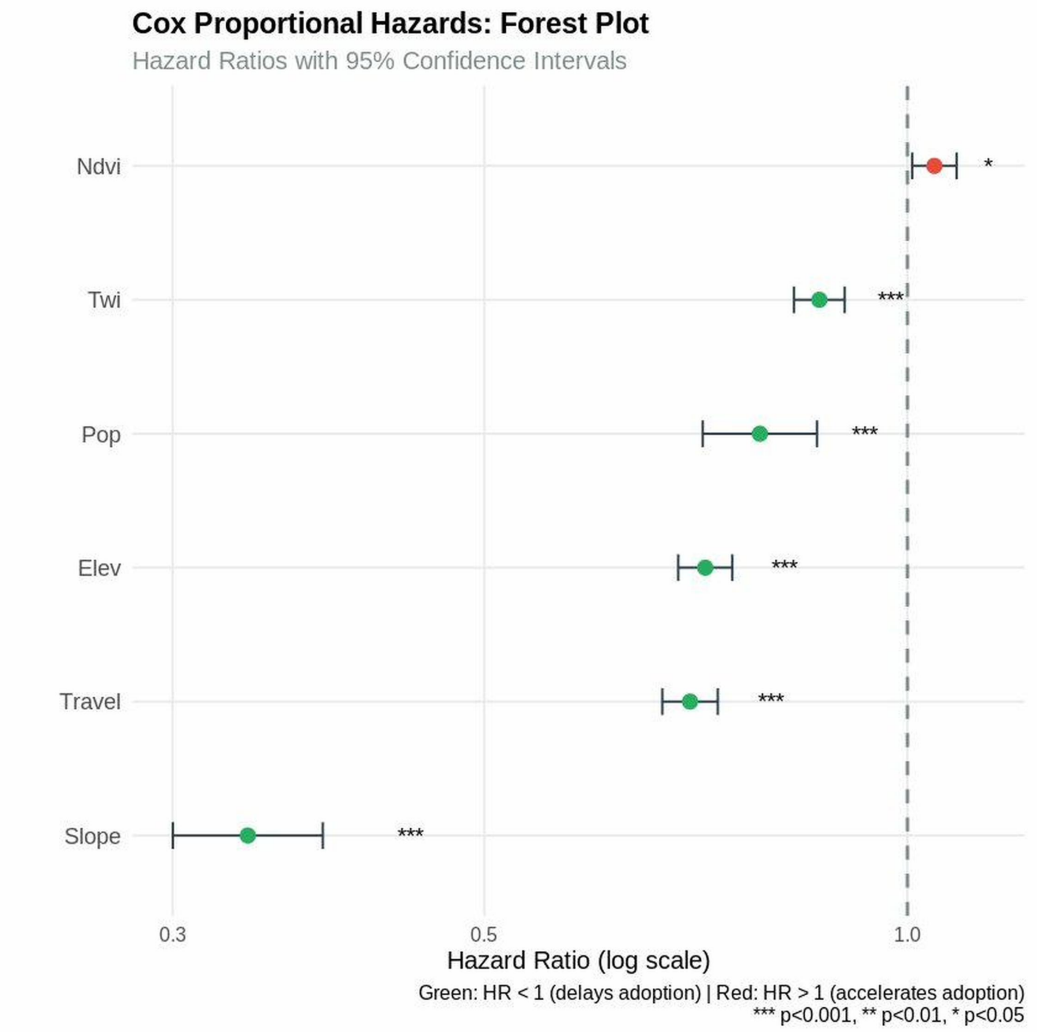

Figure 6: Forest plot of hazard ratios from the baseline Cox proportional hazards model (Table 2). Standardized coefficients with 95% confidence intervals. Green points indicate HR < 1 (delays adoption); red points indicate HR > 1 (accelerates adoption). Dashed line at HR $= 1$ indicates no effect.

Table 2: Cox proportional hazards results — baseline model with cluster-robust inference.

Variable	HR	95% CI	p (standard)	p (cluster-robust)
Slope (z)	0.339	[0.300, 0.384]	< 0.001	< 0.001
Travel time (z)	0.700	[0.669, 0.733]	< 0.001	< 0.001
Elevation (z)	0.718	[0.687, 0.751]	< 0.001	< 0.001
Pop. density (z)	0.785	[0.715, 0.862]	< 0.001	0.004
TWI (z)	0.866	[0.831, 0.902]	< 0.001	< 0.001
Baseline NDVI (z)	1.045	[1.008, 1.084]	0.017	0.164
Model fit				
N (events)	13,201 (3,201)			
Concordance	0.675 (SE = 0.005)			
Spatial clusters	377			
Avg. SE inflation	1.93×			

Notes: HR = Hazard Ratio. Variables standardized to z-scores. HR < 1 indicates slower adoption per SD increase. Cluster-robust p-values based on sandwich estimator with 377 spatial clusters. NDVI is the only variable that loses significance under cluster-robust inference.

spatial saturation of preferred sites. Travel time became more important during the boom (pioneer HR = 0.832; boom HR = 0.681; $\Delta = -18\%$), reflecting increased dependence on market networks as adoption scaled from isolated pioneers to mass installation (Fig. A1a).

The Schoenfeld residual test confirmed violation of the proportional hazards assumption for several covariates (global $\chi^2 = 181.47$, $p < 0.001$), with elevation, NDVI, travel time, and population density exhibiting significant time-dependence. This violation is expected given the pioneer–boom structural shift and is addressed by the time-stratified analysis. Reported hazard ratios from the full model represent time-averaged effects across the entire 2013–2025 period.

5.4. Diffusion mechanism: near-zero innovation coefficient

Bass diffusion model estimation yielded a striking result: the innovation coefficient approached zero ($p = 0.001$), while the imitation coefficient was substantial ($q = 0.679$), with an estimated market ceiling of $K = 4{,}026$ wells (Table 3; Fig. 7). Formal model comparison decisively favored the pure logistic specification ($p = 0$) over the full Bass model ($\Delta\text{AIC} = 18.3$) and the Gompertz model ($\Delta\text{AIC} = 18.8$), indicating that external innovation effects are not statistically distinguishable from zero (Fig. A1b).

Table 3: Bass diffusion model comparison.

Model	Parameters	p	q	K	ΔAIC
Logistic ($p = 0$)	**2**	**0**	**0.68**	**4,026**	**0**
Bass (full)	3	0.001	0.68	4,026	18.3
Gompertz	2	—	—	—	18.8

Notes: Bold indicates best-fitting model. $\Delta\text{AIC} > 10$ constitutes decisive evidence against the inferior model (Burnham and Anderson, 2002).

This finding is unprecedented in the agricultural technology diffusion literature. The estimated q/p ratio of approximately 679 exceeds by an order of magnitude the typical range of 10–50 documented in agricultural settings (Rogers, 2003) and even surpasses extreme cases such as cellular phone adoption ($q/p \approx 168$; Baptista, 2000). The near-absence of external influence (p) implies that no farmer in our sample adopted solar irrigation because of a government program, bank loan offer, or extension service recommendation. Adoption occurred exclusively through internal social learning—observation of neighbors, word-of-mouth, and informal information networks.

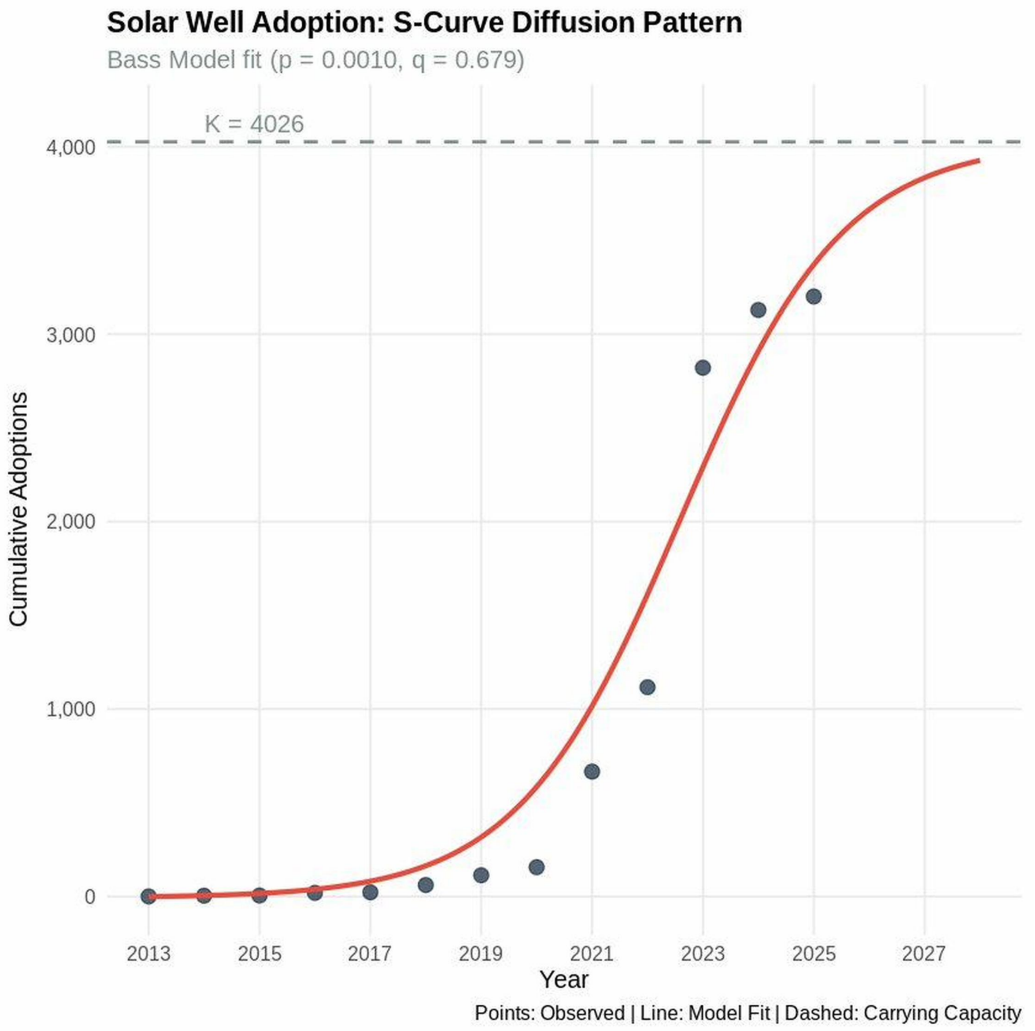

Figure 7: Cumulative adoption S-curve with fitted Bass diffusion model. The pure logistic specification ($p = 0$, $q = 0.68$, $K = 4{,}026$) is shown. Observed data points are plotted against the model fit, with the dashed horizontal line indicating the estimated carrying capacity. The absence of external influence indicates diffusion driven exclusively by imitation through informal networks.

5.5. Spatial clustering and epidemic equivalence

Moran's I confirmed strong positive spatial autocorrelation in adoption patterns ($I = 0.326$, $Z = 48.23$, $p < 0.001$). This spatial clustering—wherein adopters are located near other adopters far more than expected under spatial randomness—is consistent with the localized social learning mechanism implied by the absence of institutional diffusion channels.

Triangulation through the equivalent epidemic (SIS) model formulation yielded a growth rate of $r = 0.458$, within 33% of the Bass imitation coefficient ($q = 0.679$). The discrepancy reflects different ceiling assumptions (epidemic model: $N = 6{,}402$ vs. Bass: $K = 4{,}026$); under equivalent ceiling constraints, the two models converge. This agreement across independent modeling frameworks strengthens confidence in the social contagion interpretation: solar well diffusion in Sidi Bouzid propagates through local transmission networks analogous to an epidemic process.

5.6. Competitive diffusion: neighbor effects

To test for local saturation effects predicted by the Competitive Diffusion Framework, we estimated a Cox model incorporating the standardized count of prior wells within 5 km. The neighbor density variable was strongly significant with a hazard ratio below unity (HR = 0.606, 95% CI: 0.581–0.633, $p < 0.001$), indicating that higher local adopter density is associated with *slower* subsequent adoption (Table 4). Inclusion of the neighbor variable substantially altered other coefficients: elevation lost significance entirely

(HR = 0.996, $p = 0.87$), slope effects weakened (HR = 0.813 vs. baseline 0.339), and travel time reversed direction (HR = 1.250 vs. baseline 0.700). These changes indicate that neighbor density mediates the effect of terrain and accessibility variables—much of what appears to be a terrain effect in the baseline model reflects the clustering of prior adopters in favorable locations. The travel time reversal is particularly revealing: in the baseline model, proximity to cities appears to accelerate adoption because early adopters clustered near urban centers; once this clustering is controlled for, the residual signal captures remote farmers whose higher diesel transport costs and weaker grid access created stronger economic incentives to adopt solar pumping.

Table 4: Cox proportional hazards model with neighbor density: comparison with baseline model.

Variable	Baseline HR	Neighbor HR	95% CI	Change
Elevation (z)	0.718***	0.996	[0.944, 1.050]	Lost significance
Slope (z)	0.339***	0.813**	[0.714, 0.926]	Attenuated
Baseline NDVI (z)	1.045*	0.779***	[0.743, 0.816]	Direction reversed
Travel time (z)	0.700***	1.250***	[1.195, 1.308]	Direction reversed
Prior neighbors (z)	—	**0.606*** **	**[0.581, 0.633]**	**New variable**
Model fit				
N (events)	13,201 (3,201)			

Notes: HR = Hazard Ratio. Variables standardized to z-scores. Baseline model is Table 2. Prior neighbors = count of solar wells installed within 5 km before the focal observation. Inclusion of neighbor density substantially alters other coefficients, indicating that terrain effects in the baseline model partly reflect the spatial clustering of prior adopters.
*** $p < 0.001$, ** $p < 0.01$, * $p < 0.05$.

The negative neighbor effect resolves an apparent paradox in the aggre-

gate findings. At the population level, the Bass model indicates strong imitation ($q = 0.679$), and Moran's I confirms spatial clustering—both suggesting that neighbors accelerate adoption. Yet at the local level, higher neighbor density *slows* adoption. The Competitive Diffusion Framework reconciles these findings by distinguishing two opposing spatial forces: an *Information Effect* (positive), whereby proximity to prior adopters reduces uncertainty and demonstrates viability, operating at the aggregate level to drive the S-curve; and a *Congestion Effect* (negative), whereby spatial concentration of extraction accelerates aquifer drawdown, increases pumping depths, and raises costs for latecomers, operating at the local level to slow adoption in already-dense clusters. The sharp decline from 1,704 installations in 2023 to 380 in 2024–2025 provides temporal evidence of the phase transition our framework predicts—from Information-Effect dominance during take-off to Congestion-Effect dominance during emerging saturation.

5.7. Robustness

Several complementary checks support the validity of the core findings (Table A1 in Appendix A). Cox model coefficients were stable across six alternative specifications, with key hazard ratios for slope, elevation, and travel time exhibiting coefficients of variation below 15% (slope range: 0.339–0.448; elevation range: 0.636–0.741; travel time range: 0.692–0.766). Concordance indices ranged from 0.644 (stratified model) to 0.688 (categorical model), confirming consistent discriminative performance.

Cluster-robust standard errors, computed over 377 spatial clusters, yielded an average SE inflation of 1.93×, confirming that spatial dependence introduces meaningful uncertainty beyond what conventional standard errors capture (see Table A3 for variable-level detail). Critically, all core terrain predictors remained highly significant: slope ($p < 0.001$), elevation ($p < 0.001$), travel time ($p < 0.001$), population density ($p = 0.004$), and TWI ($p < 0.001$). The sole exception was baseline NDVI, whose marginal significance under conventional inference ($p = 0.017$) disappeared under cluster-robust estimation ($p = 0.164$). We therefore do not include NDVI among the robust predictors of adoption.

Sensitivity analysis of the Bass model ceiling parameter revealed that q varies with K assumptions (range: 0.23 at $K = 2.0\times$ observed to 1.76 at $K = 1.0\times$ observed). However, the key finding—that p is indistinguishable from zero—was robust to all tested ceiling specifications, as the logistic model ($p = 0$) was preferred under every K assumption. Bootstrap confidence intervals for p failed to converge, further confirming that the parameter is effectively zero.

6. Discussion

6.1. Theoretical contributions

This study makes two principal theoretical contributions to the technology diffusion and land use governance literatures. The first is the empirical documentation of pure social diffusion—a Bass innovation coefficient indistin-

guishable from zero—in agricultural technology adoption. While prior studies have reported low p values for green technologies (Guidolin and Guseo, 2023; Guidolin and Mortarino, 2010) and network goods (Baptista, 2000), no previous application of the Bass model to agriculture has found the external influence channel to be entirely absent.

We attribute this anomaly not to an inherent property of the technology but to the specific governance architecture of Tunisia's informal groundwater economy, confirming the prediction derived from institutional analysis in Section 3.2. The Authorization Trap severs every institutional pathway that normally generates positive p, and the Finance Law 2025's creation of a mass regularization mechanism (Article 81, Loi n° 2024-48 (Loi n° 2024-48, 2024)) constitutes legislative confirmation that this blockage was an empirical reality, not a theoretical construct. The implication extends beyond Tunisia: the near-zero innovation coefficient may characterize any context where informality excludes farmers from formal support channels—a hypothesis with broad relevance for groundwater governance in South Asia, the Sahel, and other regions where unauthorized extraction is the norm.

The second contribution is the Competitive Diffusion Framework, which resolves the apparent paradox between high aggregate imitation ($q = 0.679$, Moran's $I = 0.326$) and negative local neighbor effects (HR = 0.606). Standard diffusion theory predicts that these two findings should point in the same direction: if imitation drives adoption, proximity to prior adopters should accelerate it at every scale. Our framework distinguishes two opposing spatial

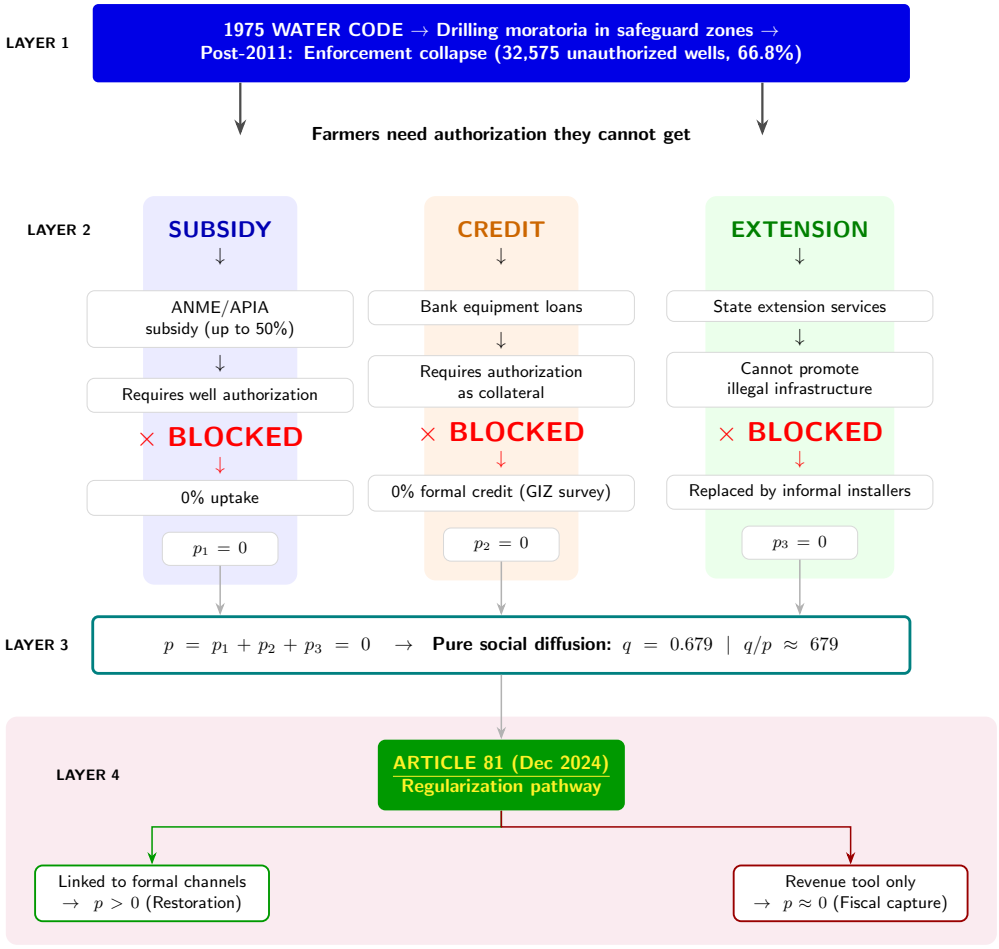

Figure 8: The Authorization Trap: governance failure pathway confirmed by the empirical finding of a near-zero innovation coefficient. Tunisia's 1975 Water Code requires drilling authorization, but regional agencies refuse permits in overexploited zones while enforcement collapsed after 2011 (32,575 unauthorized wells, 66.8% of total). Three formal technology transfer channels—subsidies (up to 50%, requiring authorization), bank credit (requiring authorization as collateral), and extension services (unable to serve illegal infrastructure)—are simultaneously blocked, producing the estimated innovation coefficient $p \approx 0$ with diffusion migrating entirely to informal imitation networks ($q = 0.679$, $q/p \approx 679$). Article 81 of the Finance Law 2025 creates a regularization pathway; whether it restores formal channels depends on linking it to subsidy eligibility, credit access, and extension services.

forces operating at different scales: an aggregate-level Information Effect that produces the S-curve and spatial clustering, and a local-level Congestion Effect through which hydrological interference, site exhaustion, and strategic delay slow adoption in already-dense clusters. This extends Bandiera and Rasul's (2006) inverse-U finding by grounding the non-linearity in the physical rivalrousness of groundwater—a mechanism absent from consumer goods contexts.

The temporal evidence supports this interpretation. The sharp collapse from 1,704 installations in 2023 to 380 in 2024–2025 is consistent with a phase transition from Information-Effect dominance to Congestion-Effect dominance. The time-stratified Cox analysis provides further evidence: the relaxation of the elevation constraint between the pioneer (HR = 0.587) and boom (HR = 0.720) periods suggests spatial saturation of preferred valley sites, pushing adoption to higher, more marginal locations where the Congestion Effect is beginning to bite.

6.2. Policy implications

The pure social diffusion finding has important implications for groundwater governance. When $p = 0$, regulators have no institutional channel through which to influence the pace, spatial distribution, or environmental footprint of technology adoption. Subsidies, permitting conditions, and extension programs—the standard policy toolkit—are inoperative because farmers never encounter them. The technology spreads through networks

invisible to the state, following its own epidemic logic.

The corollary is that adoption becomes acutely sensitive to market signals transmitted through informal networks. The collapse from 1,704 installations in 2023 to 308 in 2024—coinciding with the 2024 customs duty increase on solar equipment (see Section 3.4)—illustrates this vulnerability: with no institutional buffer mediating between price signals and adoption decisions, an external fiscal shock propagated immediately through the informal system.

This suggests that interventions aimed at steering solar irrigation adoption must work through informal channels rather than formal ones. International experience with groundwater co-management confirms that effective governance requires integrating community-level institutions into regulatory frameworks (Molle and Closas, 2020). Community leaders, early adopters, and peer networks—the very conduits through which diffusion actually operates—are more promising entry points for sustainability messaging than ministry offices or CRDA extension agents. Making aquifer stress visible to farmers through community-level reporting of declining well yields or satellite-derived vegetation anomaly indices could transform the hidden commons problem into a visible coordination game, enabling social norms against over-extraction to emerge endogenously.

Article 81 of the Finance Law 2025 creates a potentially transformative instrument: a comprehensive registry of solar wells. If linked to monitoring infrastructure—smart meters, extraction quotas tied to recharge rates, community-level water budgets—this registry could provide the first system-

atic accounting of informal extraction in a region where regulatory blindness has been the norm. However, if treated merely as a one-time revenue-generating exercise—a regularization fee without ongoing extraction conditions—Article 81 will legitimize unsustainable extraction without addressing the underlying commons dilemma. Whether regularization will restore positive innovation effects ($p > 0$) depends on whether the state links it to subsidy eligibility, extension services, and formal credit access. Without these complementary measures, Article 81 represents a recognition of past informal diffusion, not a driver of future formal diffusion.

The Competitive Diffusion Framework also offers a natural policy lever. The Congestion Effect suggests that adoption is already self-limiting in the densest clusters—precisely the zones of greatest aquifer stress. Policymakers could reinforce this natural brake by making aquifer condition information publicly available at the community level, converting the invisible resource degradation into a shared signal that amplifies the Congestion Effect before irreversible damage occurs.

6.3. Broader implications for the MENA region

The dynamics documented here are not unique to Tunisia. Across the MENA region, solar-powered irrigation is expanding into governance vacuums created by incomplete regulatory frameworks and institutional weakness. Morocco's centralized approach—establishing MASEN as a powerful coordinating agency and pursuing green industrial policy to integrate renewable

energy into national development strategy (Vidican Auktor, 2017; Kousksou et al., 2015)—offers a contrasting model in which institutional visibility is maintained over solar adoption. Jordan's experience with grid saturation from rapid rooftop solar uptake provides a cautionary parallel regarding the mismatch between adoption speed and institutional adaptation (Kiwan and Al-Ghazawi, 2022). Egypt's success with clustered development at Benban demonstrates that spatial concentration can facilitate regulation if planned proactively (World Bank, 2018). The Tunisian case, by contrast, illustrates what happens when diffusion outpaces governance entirely: by the time the state responded legislatively (December 2024), 95% of adoption had already occurred informally.

For countries facing analogous conditions—India's solar pumping expansion (Gupta, 2019; Kishore et al., 2014), sub-Saharan Africa's emerging solar irrigation sector (Falchetta et al., 2023)—the Tunisian experience provides a clear warning: institutional channels must be established before or concurrently with technology availability, not retroactively. Once p collapses to zero and diffusion migrates entirely to informal networks, the state's capacity to condition adoption on sustainability criteria is effectively lost.

6.4. Limitations and future research

Several limitations warrant consideration. First, the imitation coefficient q is sensitive to assumptions about the market ceiling K, varying from 0.23 to 1.76 across specifications. However, the key finding—that p is indis-

tinguishable from zero—is robust to all tested ceiling values. Second, the proportional hazards assumption was violated for several covariates, though time-stratified analysis addresses this by allowing effects to vary across periods; reported full-model hazard ratios represent time-averaged effects. Third, cluster-robust standard errors revealed that the NDVI effect was not robust to spatial dependence ($p = 0.164$), confirming that pre-adoption vegetation productivity should not be emphasized as a reliable predictor. Fourth, the negative neighbor effect (HR = 0.606) is consistent with both physical congestion (aquifer stress) and informational mechanisms (strategic delay, observational learning about problems)—the current data cannot distinguish between these pathways. Future research incorporating direct measurements of water table decline alongside adoption data could disentangle these mechanisms. Fifth, our governance interpretation rests on institutional analysis and legal documentation rather than direct measurement of individual farmers' subsidy applications or extension contacts. Household-level survey data linking adoption decisions to information sources would provide more direct evidence on the $p \approx 0$ finding. Sixth, the 2024–2025 decline in installations may partly reflect data truncation rather than true saturation; continued monitoring through the post-Article 81 period will reveal whether regularization restores formal channels. Seventh, installation dates are derived from the first satellite image in which a solar panel is visible, which may lag actual installation by several months depending on image acquisition frequency and cloud cover; adoption timing is therefore measured with approximately

annual precision. Eighth, control points were placed on agricultural land identified via MODIS land cover classification at 500 m resolution; this spatial granularity may misclassify some pixels at field boundaries, though the large control sample (n = 10,000) mitigates the impact of individual misclassifications. Ninth, the study is limited to a single governorate; while Sidi Bouzid is the epicenter of Tunisia's solar irrigation expansion, the extent to which these diffusion dynamics generalize to other governorates with different aquifer conditions, cropping systems, or institutional contexts remains an open empirical question.

Future research should also examine whether the Competitive Diffusion Framework applies to other rivalrous technology diffusion contexts—for example, fisheries where new harvesting technologies deplete shared stocks, or forestry where mechanized clearing creates analogous commons dilemmas. Agent-based spatial models (Berger, 2001) offer a promising simulation platform for testing these dynamics under varying institutional and resource conditions. The framework's core insight—that rivalry in the resource base transforms the relationship between adoption density and subsequent adoption from positive to negative—may prove generalizable well beyond the solar irrigation case.

7. Conclusions

This study documents a previously unobserved phenomenon in technology diffusion: the complete absence of institutional influence over the adoption of

a transformative agricultural technology. In Sidi Bouzid, Tunisia, 3,201 solar-powered irrigation wells diffused between 2013 and 2025 through pure social contagion, with no measurable contribution from subsidies, credit, or extension services. The Bass innovation coefficient approaches zero—an anomaly we trace to the Authorization Trap that systematically excludes the majority of farmers from formal support channels.

The Competitive Diffusion Framework proposed here reconciles high aggregate imitation with negative local neighbor effects by distinguishing between an Information Effect that drives the S-curve and a Congestion Effect that creates saturation pockets as groundwater stress intensifies. The sharp collapse from peak adoption in 2023 to near-cessation in 2024–2025 provides real-time evidence of this phase transition.

For policy, the message is twofold. First, governance frameworks must be established before or alongside technology availability; once diffusion migrates to informal networks, the state's capacity to condition adoption on sustainability is lost. Second, Article 81 of the Finance Law 2025 offers a rare corrective opportunity—but only if the registry it creates is leveraged for monitoring and extraction governance, not merely for revenue collection. Whether Tunisia converts a fiscal instrument into a governance instrument will determine whether the solar irrigation revolution ends as an adaptation success story or as the mechanism through which a semi-arid nation depleted its last strategic water reserves.

Data availability

Data will be made available on request.

References

Anselin, L., 1995. Local Indicators of Spatial Association—LISA. Geographical Analysis 27(2), 93–115.

Bandiera, O., Rasul, I., 2006. Social networks and technology adoption in northern Mozambique. The Economic Journal 116(514), 869–902.

Baptista, R., 2000. Do innovations diffuse faster within geographical clusters? International Journal of Industrial Organization 18(3), 515–535.

Bass, F.M., 1969. A new product growth model for consumer durables. Management Science 15(5), 215–227.

Berger, T., 2001. Agent-based spatial models applied to agriculture: a simulation tool for technology diffusion, resource use changes and policy analysis. Agricultural Economics 25(2–3), 245–260.

Breiman, L., 2001. Random forests. Machine Learning 45(1), 5–32.

Burnham, K.P., Anderson, D.R., 2002. Model Selection and Multimodel Inference: A Practical Information-Theoretic Approach, second ed. Springer, New York.

Closas, A., Rap, E., 2017. Solar-based groundwater pumping for irrigation: sustainability, policies, and limitations. Energy Policy 104, 33–37.

Conley, T.G., Udry, C.R., 2010. Learning about a new technology: pineapple in Ghana. American Economic Review 100(1), 35–69.

Edwards, E.C., 2016. What lies beneath? Aquifer heterogeneity and the economics of groundwater management. Journal of the Association of Environmental and Resource Economists 3(2), 453–491.

Elloumi, M., 2018. Tunisie : Agriculture, Le développement compromis. Éditions Nirvana, Tunis.

Falchetta, G., Semeria, F., Tuninetti, M., et al., 2023. Solar irrigation in sub-Saharan Africa: economic feasibility and development potential. Environmental Research Letters 18(9), 094044.

Foster, A.D., Rosenzweig, M.R., 1995. Learning by doing and learning from others: human capital and technical change in agriculture. Journal of Political Economy 103(6), 1176–1209.

Friedl, M.A., Sulla-Menashe, D., Tan, B., et al., 2010. MODIS Collection 5 global land cover: algorithm refinements and characterization of new datasets. Remote Sensing of Environment 114(1), 168–182.

Frija, A., Chebil, A., Speelman, S., Faysse, N., 2014. A critical assessment of groundwater governance in Tunisia. Water Policy 16(2), 358–373.

Genius, M., Koundouri, P., Nauges, C., Tzouvelekas, V., 2014. Information transmission in irrigation technology adoption and diffusion: social learning, extension services, and spatial effects. American Journal of Agricultural Economics 96(1), 328–344.

GIZ/ANME, 2019. Étude sur le pompage solaire en Tunisie: diagnostic et recommandations. Deutsche Gesellschaft für Internationale Zusammenarbeit / Agence Nationale pour la Maîtrise de l'Énergie, Tunis.

Gorelick, N., Hancher, M., Dixon, M., Ilyushchenko, S., Thau, D., Moore, R., 2017. Google Earth Engine: planetary-scale geospatial analysis for everyone. Remote Sensing of Environment 202, 18–27.

Grambsch, P.M., Therneau, T.M., 1994. Proportional hazards tests and diagnostics based on weighted residuals. Biometrika 81(3), 515–526.

Guidolin, M., Guseo, R., 2023. Innovation diffusion processes: concepts, models, and predictions. Annual Review of Statistics and Its Application 10, 451–473.

Guidolin, M., Mortarino, C., 2010. Cross-country diffusion of photovoltaic systems: modelling choices and forecasts for national adoption patterns. Technological Forecasting and Social Change 77(2), 279–296.

Gupta, E., 2019. The impact of solar water pumps on energy-water-food nexus: evidence from Rajasthan, India. Energy Policy 129, 598–609.

Hägerstrand, T., 1967. Innovation Diffusion as a Spatial Process. University of Chicago Press, Chicago.

Hardin, G., 1968. The tragedy of the commons. Science 162(3859), 1243–1248.

Hoff, H., 2011. Understanding the Nexus. Background Paper for the Bonn2011 Conference: The Water, Energy and Food Security Nexus. Stockholm Environment Institute, Stockholm.

International Renewable Energy Agency (IRENA), 2024. Renewable Power Generation Costs in 2023. IRENA, Abu Dhabi.

Kishore, A., Shah, T., Tewari, N.P., 2014. Solar irrigation pumps: farmers' experience and state policy in Rajasthan. Economic and Political Weekly 49(10), 55–62.

Kiwan, S., Al-Ghazawi, Z., 2022. Assessment of the renewable energy sector in Jordan: current status and future challenges. Results in Engineering 15, 100486.

Kousksou, T., Allouhi, A., Belattar, M., Jamil, A., El Rhafiki, T., Zeraouli, Y., 2015. Renewable energy potential and national policy directions for sustainable development in Morocco. Renewable and Sustainable Energy Reviews 47, 46–57.

Lin, D.Y., Wei, L.J., 1989. The robust inference for the Cox proportional

hazards model. Journal of the American Statistical Association 84(408), 1074–1078.

République Tunisienne, 1975. Loi n° 75-16 du 31 mars 1975, portant promulgation du Code des eaux. Journal Officiel de la République Tunisienne (JORT) n° 22 (1 avril 1975), 612.

République Tunisienne, 2023. Loi n° 2023-13 du 11 décembre 2023, portant loi de finances pour l'année 2024. Journal Officiel de la République Tunisienne (JORT) n° 144 (12 décembre 2023).

République Tunisienne, 2024. Loi n° 2024-48 du 9 décembre 2024, portant loi de finances pour l'année 2025. Journal Officiel de la République Tunisienne (JORT) n° 149 (10 décembre 2024).

Madani, K., Dinar, A., 2012. Cooperative institutions for sustainable common pool resource management: application to groundwater. Water Resources Research 48(9), W09553.

Maertens, A., Barrett, C.B., 2013. Measuring social networks' effects on agricultural technology adoption. American Journal of Agricultural Economics 95(2), 353–359.

Massiani, J., 2015. The choice of Bass model coefficients to forecast diffusion for innovative products: an empirical investigation for new automotive technologies. Research in Transportation Economics 50, 17–28.

Ministère de l'Agriculture, des Ressources Hydrauliques et de la Pêche, 2020. Annuaire Statistique. République Tunisienne, Tunis.

Molle, F., Closas, A., 2020. Co-management of groundwater: a review. WIREs Water 7(1), e1394.

Observatoire National de l'Agriculture (ONAGRI), 2023. Rapport annuel sur les ressources en eau souterraine. République Tunisienne, Tunis.

Office National de l'Huile (ONH), 2024. Bulletin mensuel des prix de l'huile d'olive. République Tunisienne, Tunis.

Ostrom, E., 1990. Governing the Commons: The Evolution of Institutions for Collective Action. Cambridge University Press, Cambridge.

Pfeiffer, L., Lin, C.-Y.C., 2014. Does efficient irrigation technology lead to reduced groundwater extraction? Empirical evidence. Journal of Environmental Economics and Management 67(2), 189–208.

Rogers, E.M., 2003. Diffusion of Innovations, fifth ed. Free Press, New York.

Sears, L., Caparelli, J., Lee, C., Pan, D., Strandberg, G., Vuu, L., Lin Lawell, C.-Y.C., 2018. Jevons' paradox and efficient irrigation technology. Sustainability 10(5), 1590.

Sultan, F., Farley, J.U., Lehmann, D.R., 1990. A meta-analysis of applications of diffusion models. Journal of Marketing Research 27(1), 70–77.

Therneau, T.M., 2023. A package for survival analysis in R. R package version 3.5-7. https://CRAN.R-project.org/package=survival.

Vidican Auktor, G., 2017. Renewable energy as a trigger for industrial development in Morocco. In: Altenburg, T., Assmann, C. (Eds.), Green Industrial Policy: Concept, Policies, Country Experiences. UN Environment / German Development Institute, Geneva/Bonn, pp. 153–165.

Weiss, D.J., Nelson, A., Gibson, H.S., et al., 2018. A global map of travel time to cities to assess inequalities in accessibility in 2015. Nature 553, 333–336.

World Bank, 2018. Maximizing Finance for Development: Egypt—Enabling Private Investment in Renewable Energy. World Bank Group, Washington, D.C. (Brief No. 125274).

Appendix A. Robustness Checks and Additional Results

Table A1: Summary of robustness checks.

Check	Result	Interpretation
Cox model stability (6 specs)	CV $< 15\%$ for core HRs	Coefficients robust across specifications
Cluster-robust SEs (377 clusters)	Avg. SE inflation 1.93×	Spatial dependence meaningful but findings hold
Core predictors under robust SEs	Slope, elevation, travel time: $p < 0.001$	Main findings robust
NDVI under robust SEs	$p = 0.017 \rightarrow p = 0.164$	Not robust; excluded from key findings
PH assumption (Schoenfeld)	Global $\chi^2 = 181.5$, $p < 0.001$	Violated; addressed by time-stratified analysis
Bass model: logistic preferred	$\Delta\text{AIC} = 18.3$ (decisive)	$p \approx 0$ strongly supported
Bootstrap CI for p	Failed to converge ($p \rightarrow 0$)	p indistinguishable from zero
K sensitivity (q range)	$q = 0.23$–1.76 across K specs	q sensitive to ceiling; $p \approx 0$ robust regardless
Moran's I	$I = 0.326$, $p < 0.001$	Spatial clustering validated
Epidemic model triangulation	$r = 0.46 \approx q = 0.68$	Independent confirmation of social contagion
Neighbor effects	HR $= 0.606$, $p < 0.001$	Congestion Effect validated

Notes: Each check is described in Section 4.4 (methods) and Section 5.7 (results). CV = coefficient of variation across six Cox model specifications (Models A–F). SE inflation = ratio of cluster-robust to conventional standard errors. ΔAIC computed relative to the best-fitting (logistic) model.

Table A2: Cox proportional hazards results by adoption period: pioneer (2013–2020) versus boom (2021–2025).

Variable	Pioneer HR ($n = 157$)	Boom HR ($n = 3{,}044$)	% Change	Interpretation
Elevation (z)	0.587	0.720	+22.7	Constraint relaxed
Slope (z)	0.427	0.400	−6.3	Stable (non-negotiable)
Baseline NDVI (z)	0.908	1.051	+15.7	Shifted direction
Travel time (z)	0.832	0.681	−18.1	Strengthened
Pop. density (z)	0.449	0.788	+75.5	Constraint relaxed

Notes: HR = Hazard Ratio. Variables standardized to z-scores. Pioneer = 2013–2020; Boom = 2021–2025. % Change = (Boom HR − Pioneer HR) / Pioneer HR × 100. A positive % change indicates a weakening constraint (HR moving toward 1.0). The slope constraint remains stable across periods ($\Delta = -6.3\%$), confirming flat terrain as a non-negotiable requirement. Elevation relaxes substantially (+22.7%), consistent with spatial saturation of preferred low-lying sites during the boom.

Table A3: Variable-level comparison of standard and cluster-robust standard errors (377 spatial clusters).

Variable	HR	SE (std)	SE (robust)	p (std)	p (robust)	Inflation
Elevation (z)	0.718	0.023	0.065	< 0.001	< 0.001	2.87×
Slope (z)	0.339	0.063	0.078	< 0.001	< 0.001	1.24×
Baseline NDVI (z)	1.045	0.019	0.032	0.017	0.164	1.71×
Travel time (z)	0.700	0.023	0.065	< 0.001	< 0.001	2.81×
Pop. density (z)	0.785	0.048	0.085	< 0.001	0.004	1.77×
TWI (z)	0.866	0.021	0.025	< 0.001	< 0.001	1.17×
					Average SE inflation:	**1.93**×

Notes: SE = standard error of log(HR). Inflation = SE(robust) / SE(std). The study area was partitioned into 377 spatial clusters based on a geographic grid. Cluster-robust variance estimates were computed using the grouped jackknife (cluster sandwich) estimator (Lin and Wei, 1989). NDVI is the only variable whose significance changes under cluster-robust inference ($p = 0.017 \rightarrow p = 0.164$), indicating that its marginal association with adoption is driven by within-cluster correlation rather than a genuine population-level effect.

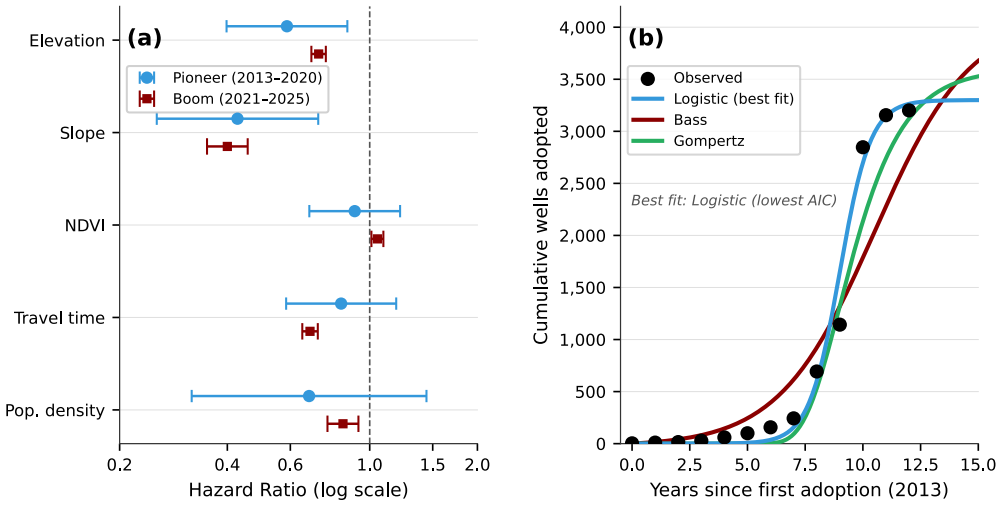

Figure A1: Robustness visualizations. (a) Cox proportional hazards ratios by adoption period, showing Pioneer (2013–2020, $n = 157$) versus Boom (2021–2025, $n = 3{,}044$) phases. Wide confidence intervals for the Pioneer period reflect limited events. The slope constraint remains stable across periods ($\Delta = -6.3\%$), while elevation relaxes substantially ($+22.7\%$). (b) Cumulative adoption S-curve with three fitted diffusion models. The logistic model ($p = 0$) provides the best fit (ΔAIC $= 18.3$ over Bass, 18.8 over Gompertz), confirming that external innovation effects are indistinguishable from zero.

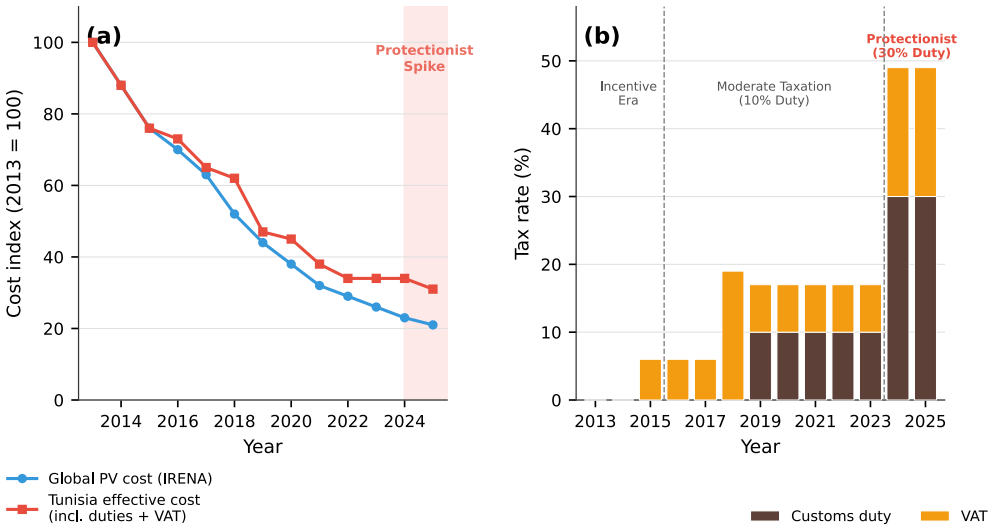

Sources: Loi de Finances 2015–2025, ANME decrees, IRENA (global PV costs)

Figure A2: Fiscal environment for solar equipment in Tunisia. (a) Global solar PV cost index (IRENA) versus Tunisia's effective cost including customs duties and VAT. The two series diverge after 2018 as domestic fiscal policy increasingly offsets global cost reductions. The 2024 customs duty tripling (10% → 30%, Article 40) creates a sharp protectionist spike. (b) Evolution of combined tax burden on imported solar equipment, showing three distinct policy eras: Incentive (0% customs duty, 2013–2015), Moderate Taxation (10% duty, 2016–2023), and Protectionist (30% duty, 2024+). Sources: Loi de Finances 2015–2025, ANME decrees, IRENA.

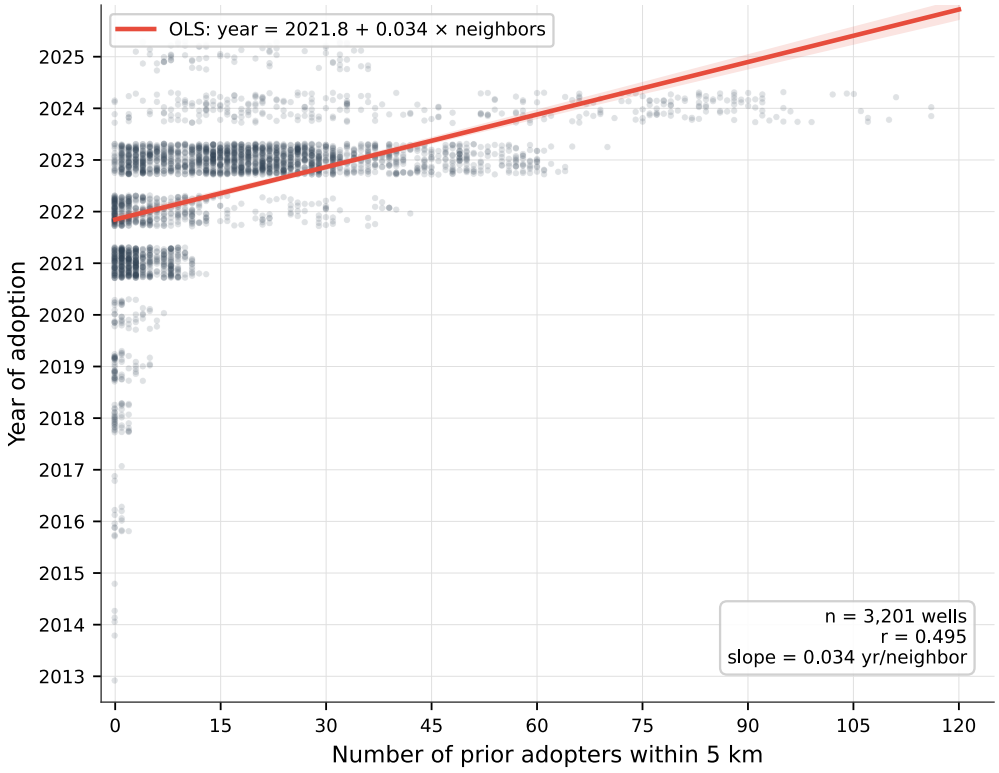

Figure A3: Social learning evidence: relationship between the number of prior adopters within 5 km and adoption year. Later adopters have systematically more prior neighbors, consistent with the Information Effect driving aggregate diffusion. The positive slope confirms that adoption clusters spatially and temporally. However, at the local level, this density simultaneously triggers the Congestion Effect (see Table 4).

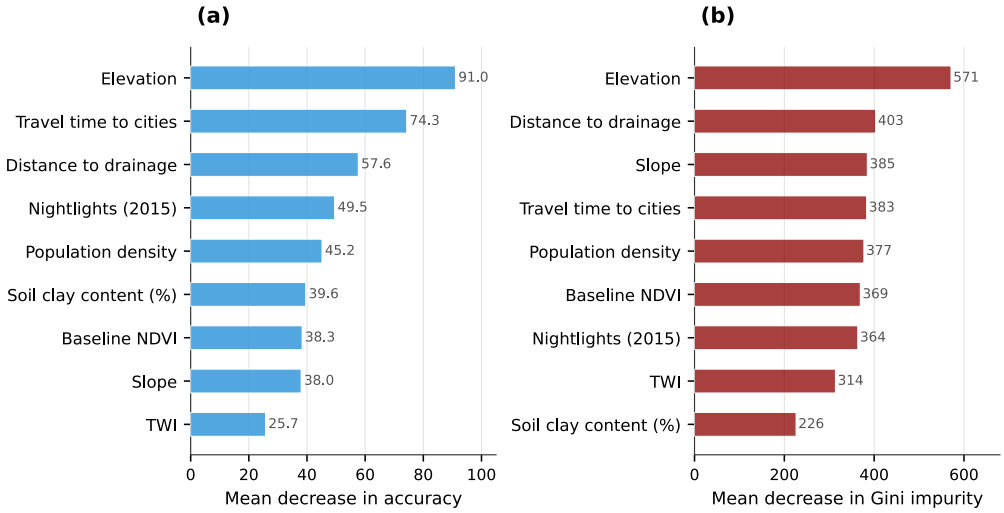

Figure A4: Random forest variable importance for well placement prediction, showing Mean Decrease in Accuracy (left) and Mean Decrease in Gini impurity (right). Elevation is the dominant predictor under both metrics. Travel time to cities and distance to drainage networks rank among the top three predictors, with their relative ordering varying by metric. These results broadly corroborate the Cox proportional hazards model while additionally identifying distance to drainage and nighttime lights as informative spatial features not included in the survival analysis.